Cross sections and excitation rates for electron collisions with heliumlike ions

A. K. Pradhan, D. W. Norcross,* and D. G. Hummer*
Joint Institute for Laboratory Astrophysics, University of Colorado and National Bureau of Standards, Boulder, Colorado 80309
(Received 23 April 1980)

We describe the techniques and the approximations used in extensive calculations for cross sections and reaction-rate parameters for electron-impact excitation of a number of heliumlike ions. All transitions involving the ground state and the $n=2$ states are considered. Calculations are made in the distorted-wave approximation using configuration-interaction wave functions to represent the target states. Autoionizing resonances in the scattering cross sections are included through bound-channel correlation-type functions and through quantum-defect-theory analysis of the reactance matrices. The resonances are shown to make considerable contributions to the cross sections and thereby, in many cases, to enhance the excitation-rate coefficients by a significant factor. This should have important consequences for practical applications in the analysis of laboratory and astrophysical plasmas. The accuracy of our approximations is also discussed.

I. INTRODUCTION

The helium isoelectronic sequence is of considerable importance in several areas of astronomy and in the diagnostics and estimation of power loss from fusion plasmas in magnetic-confinement reactors. For example, accurate data are required for the interpretation of observations from the Solar Maximum Mission (SMM) satellite for studying solar flares and related phenomena. Gabriel and Jordan[1] and Blumenthal *et al.*[2] have pointed out that the ratio of the line intensities for transitions $2\,^3S-1\,^1S$ and $2\,^3P^o-1\,^1S$ can be used to estimate the electron density N_e of a hot plasma as found, for example, in the solar corona. In fusion reactors the problem of diagnostics is similar to that in astrophysical applications. However, more important is the estimation of radiative power loss from the reactor plasma due to impurity ions, some of the most important ones being He-like.[3] For practical applications one requires accurate reaction rates for transitions produced by electron impact, over a large electron-temperature range. A typical range for astrophysical applications is 10^4–10^8 K and for fusion applications, 10^6–10^9 K. The excitation-rate coefficient for a transition between initial level i and final level j is given by

$$q_{ij}=\frac{8.63\times10^{-6}}{\omega_i T^{1/2}}\, e^{-E_{ij}/kT}\gamma_{ji}(T), \tag{1}$$

in units of $\mathrm{cm}^3\,\mathrm{sec}^{-1}$, where E_{ij} is the excitation energy, ω_i is the statistical weight of the initial level, and T is the electron temperature in K. The *rate parameter* γ, assuming a Maxwellian electron distribution, is

$$\gamma_{ji}=\int_0^\infty \Omega_{ij}\, e^{-\epsilon_j/kT}\, d\left(\frac{\epsilon_j}{kt}\right). \tag{2}$$

Ω_{ij} is the collision strength for transitions between states i and j, related to the cross section Q_{ij} by

$$Q_{ij}=\left(\frac{\Omega_{ij}}{(\omega_i\epsilon_i)}\right)(\pi a_0^2), \tag{3}$$

where ϵ_i is the incident-electron kinetic energy relative to level i in rydbergs and a_0 is the Bohr radius.

In the low-energy region where low partial waves dominate the cross section, either the close-coupling (CC) or the distorted-wave (DW) approximation is often employed in scattering calculations. For multiply charged ions, the coupling between different channels is usually weak and the DW approximation is often very good in comparison with the more elaborate CC approximation. As we shall show, this is particularly true for He-like ions; consequently we employ the DW approximation in the present work. In the high-energy region *and* for high partial waves, we use the Coulomb-Bethe (CB) approximation[4] to compute the partial contributions to the cross sections. Also, for multiply charged ions it is important to consider the autoionizing resonances in the scattering cross sections in the near-threshold regions.[5] The resonant contribution is often larger (in some cases considerably so) than the background or nonresonant contribution to the cross section. In one previous calculation,[6] an enhancement due to resonances was seen that is very large indeed, up to a factor of 30. We analyze the resonance structures using accurate numerical interpolation methods and quantum-defect theory (QDT) as described by Seaton.[7]

Detailed collision strengths and rate coefficients have been calculated for a number of ions. In this paper we present and discuss illustrative results for Be III, C V, O VII, and Fe XXV. Rate coef-

ficients for practical applications in the temperature range 10^4–10^9 K will be published elsewhere for the following ions: BeIII, CV, OVII, NeIX, SiXIII, CaXIX, FeXXV, SeXXXIII, and MoXLI.

II. THEORY AND METHOD

The general formulation for the computation of electron-ion collision cross sections in the DW and CC approximations has been discussed by Eissner and Seaton,[8] and incorporated in the computer code discussed by Eissner.[9] We present below an outline of the DW method along with certain special features included in the present work.

The total wave function for the e + ion system for a particular scattering symmetry $\mathrm{SL}\pi$ may be written

$$\Psi^{\mathrm{SL}\pi} = \sum_{i=1}^{\mathrm{NCHF}} \theta_i + \sum_{j=1}^{\mathrm{NCHB}} c_j \Phi_j \ . \tag{4}$$

The first summation includes all the "free" channels, NCHF, where

$$\theta_i = A\{\phi(S_i L_i) F_i(r, \epsilon_i)\} \tag{5}$$

are the "free" channel functions with $\phi(S_i L_i)$ as the target ionic wave function for the state $S_i L_i$, F_i is the free-electron radial wave function, and A is the antisymmetrization operator (angular variables have been omitted for convenience). The second summation in (4) includes all "bound" channels, NCHB, where the bound-channel function may be expressed as

$$\Phi_j = A\{\phi(S_i L_i) P_\alpha(nl)\} \ . \tag{6}$$

The functions $\phi(S_i L_i)$ and Φ_j are constructed from the *same* set of one-electron orbitals $\{P_\alpha(nl)\}$, and thus Φ_j has the form of a bound state of the e + ion system. The Φ_j are included in order that the orthogonality conditions $(F_i | P_\alpha) = 0$ may be imposed on the computed free-electron wave functions,[10] but also represent short-range correlation effects. The c_j coefficients are determined by the variational principle. The basis set of one-electron radial orbital wave functions $\{P_\alpha(nl)\}$ is calculated in a scaled Thomas-Fermi-Dirac (TFD) potential $V(\lambda_l, r)$ in which the parameters λ_l are scaled to produce good eigenenergies and oscillator strengths for the target states.[11]

Applying the Kohn variational principle to the total antisymmetrized vector-coupled wave function denoted by (4), one obtains in the DW approximation

$$\underline{R}^{\mathrm{DW}} = -(\underline{\Psi} | H - E | \underline{\Psi}) \ , \tag{7}$$

where $\underline{R}$ is the reactance matrix and H is the $(N+1)$-electron Hamiltonian. Equation (7) may be rewritten, for the individual $\underline{R}$ matrix elements, as

$$R^{\mathrm{DW}}_{ii'} = -\{F_i | (h_i - \epsilon_i)\delta_{ii'} + [\underline{W} - \underline{U}^\dagger (\mathcal{H} - E)^{-1} \underline{U}]_{ii'} | F_{i'}\} , \tag{8}$$

where h_i is the one-electron Hamiltonian operator and $\underline{W}$ and $\underline{U}$ are potential operators. The DW radial functions $F_i^{\mathrm{DW}}(r, \epsilon_i)$ are also calculated in the statistical model potential $V(\lambda_l, r)$ mentioned earlier, i.e.,

$$\left(\frac{d^2}{dr^2} - \frac{l(l+1)}{r^2} + 2V(\lambda_l, r) + \epsilon_i\right) F_{il}^{\mathrm{DW}}(r, \epsilon_i) = 0 \ . \tag{9}$$

The parameter λ_l corresponding to the free-electron waves F_{il} may either be chosen to be the same as those for the target orbitals $\{P_\alpha(nl)\}$ or may be varied to minimize selected $\underline{R}$ matrix elements.

In Eq. (8) the matrix $\mathcal{H}$ has elements given by

$$\mathcal{H}_{jj'} = (\Phi_j | H | \Phi_{j'}) \ . \tag{10}$$

Thus the last term in (8) has the form of an effective optical potential for states not included in the first term of the expansion (4), and it follows that $\underline{R}$ may have poles at eigenvalues of $\mathcal{H}$ that correspond to autoionizing states of the e^+-ion system.[12] A similar approach in the CC approximation has been adopted to obtain resonance structures in excitation of H-like ions.[12,13] These studies, in particular that of Hayes and Seaton,[13] showed that quite good results could be obtained *without* the necessity of including the parent states of the resonances in the first term of expansion (4). In the present work, as in that of Hayes and Seaton, the functions Φ_j are composed of "spectroscopic" orbitals, and are thus easily tailored to include functions corresponding to particular autoionizing states of interest.

In order to obtain the detailed resonance structures one requires the cross section at a large number of points. Since direct computations are very expensive, we use numerical techniques and QDT to analyze $\underline{R}$ matrices which then yield the detailed collision strengths and cross sections. A computer program RANAL has been written for this purpose[14] and has the following basic features. In energy regions where resonance structures appear explicitly in the calculated $\underline{R}$ matrix elements, they are fitted to polynomials in energy, along with poles representing resonances, i.e.,

$$R_{ii'}(\epsilon) = \sum_{k=1}^{\mathrm{IP}} a_k \epsilon^{k-1} + \sum_{n=1}^{\mathrm{IQ}} \frac{a_{\mathrm{IP}+n}}{(\epsilon - \epsilon_n)} \ , \tag{11}$$

where a_k are the expansion coefficients, IP is the degree of the polynomial, IQ is the number of poles, and ϵ_n are the pole positions. The numeri-

cal fit (11) may be made arbitrarily accurate by including a sufficient number of energies. The parameters IP, IQ, and ϵ_n are required to be the same for all $\underline{R}$ matrix elements for a given $SL\pi$.

RANAL may also be used to analyze resonance structures in energy regions below given thresholds using QDT, thereby obviating scattering calculations in such regions. $\underline{R}$ matrices computed above the threshold, in the region where all channels included in the calculations are open and the $\underline{R}$ matrices are slowly varying, are extrapolated below threshold where some channels are open and some closed, using

$$\underline{\bar{R}}^{<} = \underline{R}^{>}_{oo} - \underline{R}^{>}_{oc}(\underline{R}^{>}_{cc} + \tan \pi \nu_c)^{-1}\, \underline{R}^{>}_{co} \ , \tag{12}$$

where o refers to open channels and c to closed channels, and ν_c is the effective quantum number for the closed channels. $\underline{\bar{R}}^{<}$ is the reactance matrix below threshold for the channels that remain open. $\underline{R}^{>}_{oo}$, $\underline{R}^{>}_{oc}$, $\underline{R}^{>}_{co}$, and $\underline{R}^{>}_{cc}$ are obtained on analytic continuation of the $\underline{R}$ matrix from above threshold that is partitioned according to the scheme

$$\underline{R}^{>} = \begin{pmatrix} \underline{R}^{>}_{oo} & \underline{R}^{>}_{oc} \\ \underline{R}^{>}_{co} & \underline{R}^{>}_{cc} \end{pmatrix} . \tag{13}$$

After computing the reactance matrices as continuous functions of energy, we obtain the scattering matrices $\underline{S}$ and collision strengths Ω from the following expressions:

$$\underline{S} = (i - \underline{R})(i + \underline{R})^{-1} \tag{14}$$

and

$$\Omega(S_i L_i, S_{i'} L_{i'}) = \sum_{SL\pi} \sum_{ll'} \Omega_{SL\pi}(S_i L_i l, S_{i'} L_{i'} l') \ , \tag{15}$$

$$\Omega(S_i L_i l, S_{i'} L_{i'}, l') = \tfrac{1}{2}(2S+1)(2L+1) \times |\underline{S}_{SL\pi}(S_i L_i l, S_{i'} L_{i'} l')|^2 \ , \tag{16}$$

where $S_i L_i$ and $S_{i'} L_{i'}$ denote initial and final target states, and l and l' denote incoming and outgoing partial waves, respectively. Excitation-rate coefficients are computed from Eqs. (1) and (2).

III. WAVE-FUNCTION REPRESENTATION

It is important first of all to obtain good representations for wave functions of the target states of the ion. In the application of the variational principle for $\underline{R}$, exact eigenfunctions for the target are assumed, and therefore any error would influence to first order the error in the calculated $\underline{R}$ matrices. In our calculations we employ target wave functions obtained from a configuration-interaction (CI) expansion.

We are interested in transitions among the ground state and the states of the $n = 2$ complex, i.e., $1\,^1S$, $2\,^3S$, $2\,^1S$, $2\,^3P^o$ and $2\,^1P^o$. The configuration expansion used for all these states is

$$1s^2,\ 1s2s,\ 1s3s,\ 2s^2,\ 2p^2, \quad \text{even parity}$$

$$1s2p,\ 1s3p,\ 2s2p,\ 2p3d, \quad \text{odd parity}.$$

The one-electron orbitals $\{1s,\ 2s,\ 2p,\ 3s,\ 3p,\ 3d\}$ are computed in the scaled TFD potential $V(\lambda_l, r)$ where the λ_l are adjusted until (a) the eigenenergies of the target states and (b) the (dipole-length) oscillator strengths for allowed transitions between target states are in good agreement with accepted values. The oscillator strengths indicate the accuracy of the ionic wave functions. In Tables I and II we give the computed energies and oscillator strengths, respectively, and compare these with data from Weiss[15] (for $Z \leq 10$) and Ermolaev and Jones.[16] The values of the scaling parameters λ_l are also given in Table II.

We chose $\boldsymbol{\lambda}_d = 1.0$ for all ions under consideration. The $3d$ orbital and the configuration $2p3d$ were introduced in order to generate additional correlation functions of the type $\Phi(nln'l'3d)$, and not for CI with the target states, the latter effect being negligible. The eigenvalues of $\mathcal{H}$ depend on the amount of CI included within the set $\{\Phi_j\}$. It is therefore necessary to include a sufficient number of these functions to permit accurate computation of the positions of the bound states and the quasibound states (corresponding to resonances) of the (e + ion) system. As an example we give below the total wave function of the system for symmetry $SL\pi = {}^2S$:

$$\begin{aligned}\Psi(^2S) = &[\theta(1\,^1Sk^2s) + \theta(2\,^3Sk^2s) + \theta(2\,^1Sk^2s) + \theta(2\,^3P^o k^2p) + \theta(2\,^1P^o k^2p)] \\ &+ [c_1\Phi(1s2p^2) + c_2\Phi(1s2p3p) + c_3\Phi(1s3p^2) + c_4\Phi(2s2p^2) + c_5\Phi(2s2p3p) + c_6\Phi(1s^22s) \\ &+ c_7\Phi(1s2s^2) + c_8\Phi(1s2s3s) + c_9\Phi(1s^23s) + c_{10}\Phi(1s3s^2) + c_{11}\Phi(2s^23s) + c_{12}\Phi(2p^23s) \\ &+ c_{13}\Phi(1s3d^2) + c_{14}\Phi(2s3d^2) + c_{15}\Phi(3s3d^2) + c_{16}\Phi(2p^23d) + c_{17}\Phi(2p3p3d)] \ ,\end{aligned}$$

TABLE I. Total energies for the ground states and excitation energies for the $n=2$ states (rydbergs) in He-like ions relative to 1^1S.

	1^1S		2^3S		2^1S		2^3P^o		2^1P^o	
	Others [a]	Present	Others	Present	Others	Present	Others	Present	Others	Present
Be III	27.3111	27.2238	8.7204	8.7168	8.9348	8.9414	8.952	8.9612	9.0952	9.0896
C V	64.8125	64.7242	21.9724	21.9710	22.3572	22.3685	22.3578	22.3691	22.6318	22.6258
O VII	118.3132	118.2244	41.2244	41.2239	41.7824	41.7957	41.7606	41.7744	42.1700	42.1637
Ne IX	187.8136	187.7246	66.4762	66.4763	67.2032	67.2230	67.1640	67.1786	67.7088	67.7023
Si XIII	374.8141	374.7250	134.980	134.981	136.061	136.078	135.970	135.986	136.787	136.780
Ca XIX	775.3145	775.2254	282.735	282.737	284.342	284.359	284.179	284.196	285.405	285.398
Fe XXV	1319.8147	1319.7260	484.419	484.492	486.624	486.641	486.389	486.405	488.023	488.016
Se XXXIII	2269.8148	2269.7270	837.498	837.499	840.333	840.350	840.001	840.017	842.181	842.173
Mo XLI	3475.8149	3475.7280	1286.51	1286.51	1290.04	1290.06	1289.61	1289.63	1292.34	1292.33

[a] Weiss (Ref. 15), for ions up to and including Ne IX, and Ermolaev and Jones (Ref. 16) for the remainder.

where k^2 is the kinetic energy of the scattered electron. For the ^2S symmetry we have also included the $3d^2$ configuration in the target since it was found that the state $1s3p^2(^2S)$ interacts strongly with the bound-channel configurations of the type $(ns3d^2)$.

The eigenvalue spectrum of $\mathcal{H}$ was studied in detail for each ion and scattering symmetry considered, using the program SUPERSTRUCTURE .[11] All eigenvalues corresponding to singly excited bound states of the e + ion system (e.g., Φ_j for $j=6$ and 9 in the above example for $SL\pi = {}^2S$) occurred at approximately the correct positions. All eigenvalues corresponding to members of the rydberg series of autoionizing states converging on states of the $n=2$ complex (e.g., $j=1$, 2, 7, and 8) occurred below the $2\,^3S$ state. All eigenvalues corresponding to autoionizing states in the series converging on the $n=3$ complex ($j=3$, 10, and 13), and no others, occurred between the $2\,^1P^o$ and the $3\,^3S$ states. All other eigenvalues corresponding to more highly excited states ($j=4$, 5, 11, 12, and 14–17) occurred at much higher energies. These latter are considered unreliable, since the parent states are not well represented in the specification of the target states, and these energies were avoided in the scattering calculations.

The accuracy of the computed energies for the resonance states may be estimated by comparing the computed eigenenergies for some doubly excited bound states with the results of more sophisticated calculations by other workers. In Table III we compare the total energies and oscillator strengths for some states of e + Be III, i.e., Be II. It is seen from Table III that our values are slightly higher than the values obtained by others.[17,18] The reason for the discrepancy are that (a) the set of functions $\{\Phi_j\}$ included is not fully complete, but one that is automatically generated by our DW computer code, given the target configurations[9] and (b) the one-electron orbitals used are for the target ion and not for the e + ion system. Condition (b) becomes less and less significant as the ion-charge increases. However, we may conclude from Table III that the errors in the positions of the resonances $1s3l3l'$ in the computed cross sections should not exceed 1 or 2%.

In all there are 12 states of the type $1s3l3l'$ that would appear as autoionizing resonances (restricting l, l' to the s, p, and d waves) in the present approximation. The calculated energies of most of these states for all ions considered in this work are given in Table IV. These are obviously a very few of the infinite number of resonances present below the $n=3$ states, i.e., $1s3lnl'$ type. We recognize this limitation and, as explained later, we provide an estimate of the effect of the remainder

TABLE II. Dipole-length oscillator strengths and scaling parameters for the TFD potential.

	$1^1S-2^1P^o$		$2^1S-2^1P^o$		$2^3S-2^3P^o$				
	Present	Ref. 15	Present	Ref. 15	Present	Ref. 15	λ_s	λ_p	λ_d
Be III	0.585	0.552	0.147	0.149	0.226	0.213	0.986	0.642	1.0
C V	0.675	0.647	0.092	0.093	0.136	0.131	0.991	0.776	1.0
O VII	0.717	0.694	0.067	0.068	0.097	0.095	0.993	0.820	1.0
Ne IX	0.741	0.723	0.053	0.053	0.0076	0.0074	0.994	0.830	1.0
Si XIII	0.768	0.754	0.037	0.037	0.053	0.052	0.996	0.834	1.0
Ca XIX	0.788	0.788	0.026	0.026	0.036	0.035	0.997	0.835	1.0
Fe XXV	0.798	0.791	0.020	0.020	0.027	0.027	0.998	0.836	1.0
Se XXXIII	0.806	0.801	0.015	0.015	0.021	0.020	0.998	0.836	1.0
Mo XLI	0.811	0.807	0.012	0.012	0.017	0.017	0.999	0.837	1.0

of the resonances on the cross sections and rate coefficients.

IV. SCATTERING COMPUTATIONS

The different total spin and angular momenta and parity ($SL\pi$) states of the e + ion system are a result of coupling the incident free-electron partial waves l with the target state $S_i L_i$ of the ion; i.e., we may denote a given channel for a particular $SL\pi$ as $S_i L_i l\ SL\pi$. We need consider only the low partial waves in the detailed resonance structures since the resonances due to high angular momenta (in practice $l > 3$) are expected to be very narrow and therefore negligible. For partial waves with $l, l' < 4$, only five $SL\pi$ states (^2S, $^2P^o$, ^2D, $^2F^o$, and ^2G) contribute to transitions involving the $n = 2$ states in He-like ions. Two exceptions are the transitions $2^3S-2^3P^o$ and $2^3P^o - 2^1P^o$, which have additional contributions from the $SL\pi$ states ^4S, $^4P^o$, ^4D, and $^4F^o$, and ^2P, $^2D^o$, and ^2F, respectively. We carry out detailed resonance analysis for the symmetries ^2S, $^2P^o$, ^2D, $^2F^o$. Resonances are not taken into account for the remainder of the $SL\pi$ states. Certainly for the quartet symmetries contributing to $2^3S-2^3P^o$ this is a reasonable approximation, since the resonant contribution is expected to be small. The distorted-wave radial functions for the free electron

TABLE III. Total energies (rydbergs) of some states of Be II.

State	Others	Present
$1s2p^2\,^2P$	−19.586 [a]	−19.486
$1s2p^2\,^2D$	−19.582 [a]	−19.536
$1s2s2p\,^4P^o$	−20.126 [b]	−20.048
$1s2s3p\,^4P^o$	−19.117 [b]	−19.000
$1s2p3s\,^4P^o$	−18.911 [b]	−18.840
$1s2p^2\,^4P$	−19.738 [b]	−19.652
$1s2p3p\,^4P$	−18.846 [b]	−18.691
$1s2s3s\,^4S$	−19.235 [b]	−19.138
$1s2p3p\,^4S$	−18.918 [b]	−18.7231

[a] Fox and Dalgarno, Ref. 17.
[b] Holöien and Geltman, Ref. 18.

$F_l^{\mathrm{DW}}(r, \epsilon)$ were calculated in the TFD potential with scaling parameters λ_l chosen to be the same as for the target orbitals $P_\alpha(n, l)$. A study[19] of the effect of the dependence on λ_l for the free waves for C V indicated that careful optimization of this parameter could lead to changes of at most 15% near thresholds. However, since in the present work we find that away from poles of $\mathcal{K}$, $|R_{ii'}| \ll 1$ for most of the $SL\pi$ states, we forego the optimization procedure. The condition $|R_{ii'}| \ll 1$ is also necessary for the validity of the DW approximation.

For $4 < l, l' \leq 15$ we computed the collision strengths in the DW approximation but without resonance analysis and without including the $3d$ configurations (this does not induce any significant errors since the $3d$ configurations in the total wave-function expansion do not influence the background collision strengths appreciably and are introduced solely for term correlation.) Partial waves up to $l, l' = 15$ were sufficient to complete the summation for all forbidden and intercombination-type transitions. However, for the optically allowed transitions it was necessary to carry out the sum over higher partial waves. The Coulomb-Bethe approximation described by Burgess[4(b)] and Burgess and Sheorey[20] was used to compute the contributions from $15 < l, l' \leq \infty$. According to the nature of the computations, the energy range from threshold to ∞ was divided into three separate intervals as follows: (i) threshold-2^1P^o, (ii) $2^1P^o - 3^3S$, and (iii) $3^3S-\infty$. The threshold in (i) may be the threshold of excitation for any one of the transitions.

In interval (i) we have several interacting rydberg series of resonances converging on different levels of the $n = 2$ complex (see Fig. 1). All computations in interval (i) were carried out using the program RANAL.[14] The detailed collision strengths in this region $[E < E(2^1P^o)]$ were obtained on QDT extrapolation of the $\underline{R}$ matrices computed just above the 2^1P^o threshold where they were found to be slowly varying. We also computed collision strengths averaged over res-

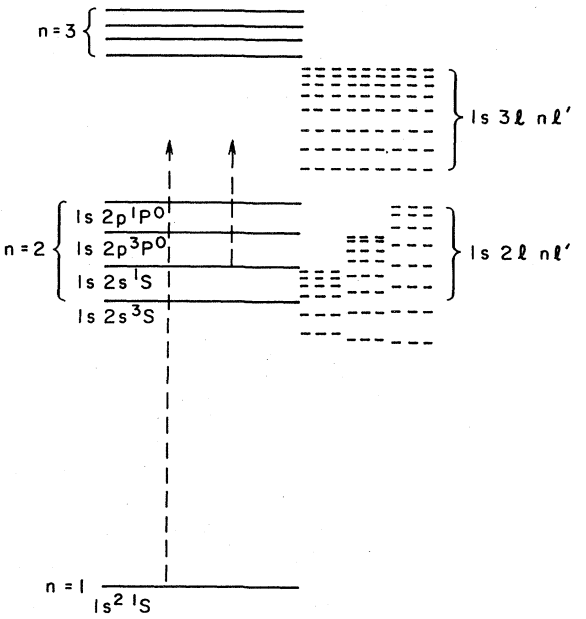

FIG. 1. Schematic energy-level diagram for He-like ions. For OVII and ions of higher charge, the $1s2s\,^1S$ lies higher than the $1s2p\,^3P^o$.

onances, employing relations from QDT developed by Gailitis (see Ref. 6), in regions just below a given threshold where the resonance series converge. Intervals of the type (i) are further subdivided into two roughly equal parts; in the first, we computed collision strengths including detailed resonance structures, and in the second we computed the Gailitis-averaged collision strengths.

In interval (ii), we calculated $\underline{R}$ matrices at a number of points sufficient to allow numerical interpolation between resonance structures of the $1s3l3l'$ complex using (11). The $\underline{R}$ matrices were fitted and the collision strengths were calculated at a fairly large number of points by RANAL. The energies at which the $\underline{R}$ matrices were calculated directly using the DW program were chosen to be in the vicinity of the resonance positions given in Table IV. Generally, approximately five points were required in order to fit each resonance. Once the fit for the $\underline{R}$ matrices has been obtained, detailed collision strengths may be computed at any number of energies.

In interval (iii) collision strengths were computed at a small number of energies up to approximately five times the threshold energy for the excitation of the ground state to $n=2$ states. We denote this last energy by ϵ_0. With increasing energy, the collision strengths for forbidden and intercombination transitions usually decrease according to power-law form. Therefore, for such transitions we fit the collision strengths to an expression of the type $\Omega = a\epsilon^{-b}$ $(b>0)$. For optically allowed transitions the collision strength may also be fitted to the same form (with $b<0$), but at sufficiently high energies they assume the asymptotic Bethe form, i.e., $\Omega \sim \ln\epsilon$. Therefore for optically allowed transitions we matched $\Omega = a\epsilon^{-b}$ $(b<0)$ to the form $(c\ln\epsilon + d)$ where the coefficients c and d were obtained by matching both the function and the derivative at the energy ϵ_0. In the present case this procedure is particularly valid since in the high-energy region the major contribution to the collision strengths for allowed transitions comes from partial waves $l>15$, which we computed in the CB approximation. Recent experimental results of Taylor *et al.*[21] for Be^+ indicate that the measured values assume the Bethe form for energies higher than about five times threshold (this may not be true in general). The contribution to the rate parameter γ from the energy range ϵ_0 to ∞ is then

$$\gamma(\epsilon_0 - \infty) = e^{-\epsilon_0/kT}(c\ln\epsilon_0 + d) + cE_1(\epsilon_0/kT)\ , \quad (17)$$

where $c\ln\epsilon_0 + d = \Omega(\epsilon_0)$ and E_1 is the exponential-integral function $\int_t^\infty e^{-t}t^{-1}dt$. Using these fitting

TABLE IV. Energies (rydbergs) for autoionizing states of the type $1s3l3l'$ relative to 1^1S.

Designation	Be III	C V	O VII	Ne IX	Si XIII	C XIX	Fe XXV	Se XXXIII	Mo XLI
$1s3s^2\,^2S$	9.5139	23.5622	43.8324	70.3246	141.9753	296.1179	506.2604	873.5617	1340.4182
$1s3s3p\,^2P^o$	9.6122	23.7293	44.0676	70.6280	142.4143	296.7605	507.1067	874.6796	1341.8077
$1s3p^2\,^2D$	9.6232	23.7442	44.9878	70.6537	142.4519	296.8160	507.1802	874.7771	1341.9292
$1s3s3p\,^2P^o$	9.6565	23.7969	44.1599	70.7453	142.5823	297.0044	507.4265	875.1007	1342.3300
$1s3s3d\,^2D$	9.7220	23.9079	44.3156	70.9455	142.8715	297.4271	507.9827	875.8347	1342.2419
$1s3p3d\,^2F^o$	9.7304	23.9343	44.3595	71.0067	142.0672	297.5744	508.1818	876.1029	1343.5791
$1s3p^2\,^2S$	9.7559	23.976	44.419	71.0840	143.0803	297.7414	508.4024	876.3951	1343.9430
$1s3p3d\,^2P^o$	9.8125	24.0724	44.5532	71.2559	143.3270	298.1001	508.8732	877.0152	1344.7125
$1s3s3d\,^2D$	9.8625	24.1412	44.6402	71.3610	143.4681	298.2947	509.1210	877.3340	1345.1021
$1s3p3d\,^2F^o$	9.8754	24.1780	44.7013	71.4462	143.6017	298.5012	509.4005	877.7107	1345.5761
$1s3p3d\,^2P^o$	9.9888	24.3516	44.9339	71.7376	144.0102	299.0848	510.1590	878.7023	1346.8007
$1s3d^2\,^2S$	10.1216	24.5747	45.2496	72.1467	144.6070	299.9641	511.3212	880.2419	1348.7180

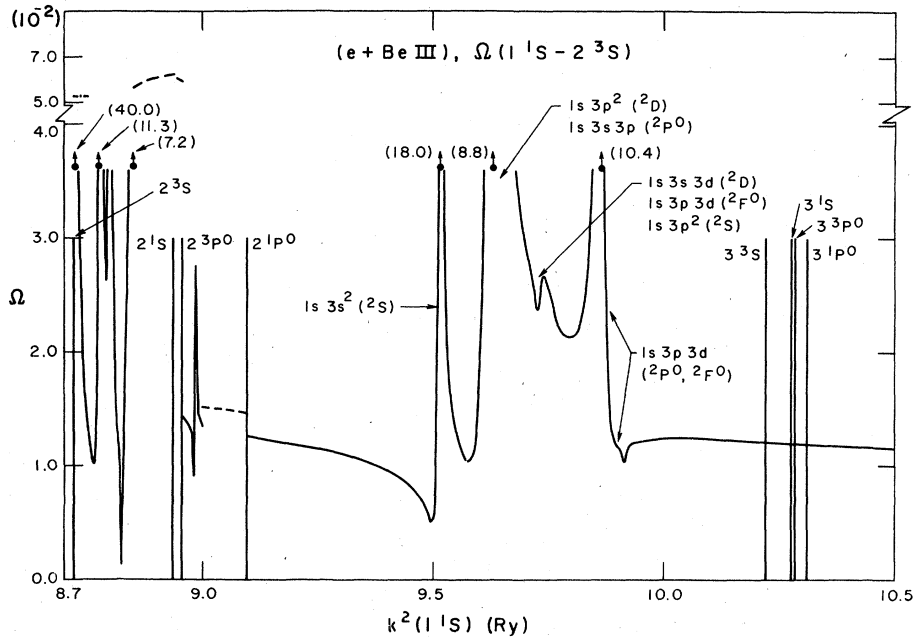

FIG. 2. Collision strength for the forbidden transition 1^1S–2^3S in Be III. $k^2(1^1S)$ is the free-electron energy relative to 1^1S.

formulas one can compute the contributions to γ from the nonresonant high-energy region.

V. RESULTS AND DISCUSSION

In this section we present selected results for collision strengths and rate parameters in order to illustrate some of the essential features.

A. Collision strenghts

The collision strengths are computed for each different $SL\pi$ state and the collision strength for a given transition (e.g., Fig. 2) is obtained by summing over all contributing $SL\pi$ states. Figure 2 shows the collision strength for the *forbidden* transition 1^1S–2^3S in Be III. Above the excitation threshold 2^3S we have several closed channels belonging to the levels 2^1S, 2^3P^o, and 2^1P^o. These channels are of the type $2(S_i L_i)nl$ $(l<4)$ and the $\underline{R}$ matrix elements corresponding to them were obtained by extrapolating from the open-channel region. The mutual interaction between various rydberg resonance series gives rise to the structure seen just above the 2^3S threshold. The approximate heights of some of the resonances are given in brackets and are seen to be quite large. For example, a numerical average over the small region just above the 2^3S threshold is indicated by -•- and its value is over four times the background collision strength above the 2^1P^o threshold. The dashed line below the 2^1S threshold represents the Gailitis-averaged collision strength in that region and is roughly the same as the numerical average. At the 2^3P^o threshold we have a large drop in the collision strength due to redistribution of flux into the newly opened 2^3P^o channels. The resonance enhancement below the 2^3P^o is large due to the strong coupling between the initial and the final states 1^1S and 2^2S, and the 2^3P^o. A much smaller Gailitis jump is seen at the 2^1P^o threshold and an almost negligible one at the 2^1S. The magnitude of the jump when a threshold is crossed reflects the strength of coupling to that state. The decrease in the effective cross section is due to the fact that the autoionizing resonances converging onto a threshold enhance the cross section below the threshold only and no longer contribute to it once the corresponding channels become open.

Between the $n=2$ and 3 complexes we have the $1s3l3l'$ group of resonances whose structures were obtained on numerical fitting of the $\underline{R}$ matrices in this region. It may be seen that there is considerable overlap between various members of the group. As mentioned earlier the $1s3l3l'$ group corresponds only to lowest members of the series $1s3lnl'$. The absence of the higher members implies that we obtain only the background collision strength in the region between the $1s3l3l'$ and the $n=3$ complex. We emphasize that since the $n=3$ states are not included in the total wave-function expansion (4), these resonances are not due to

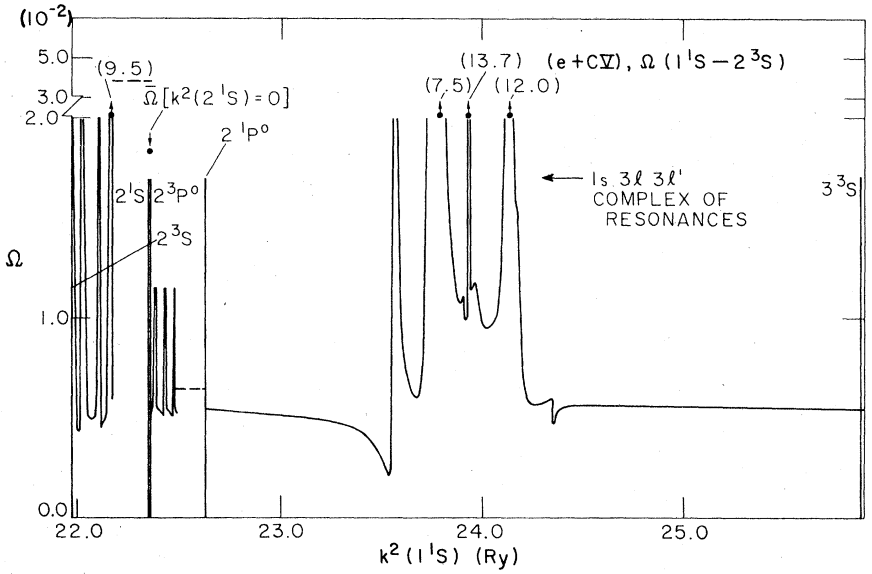

FIG. 3. Collision strength for the forbidden transition 1^1S–2^3S in C V. $\bar{\Omega}\,[k^2(2^1S)=0]$ is the averaged collision strength at the 2^1S threshold.

"closed"-channel functions belonging to the set $\{\theta_i\}$ but arise from the bound channels of the set $\{\Phi_j\}$.

In Fig. 3 we give the collision strengths for C V, also for the forbidden transition 1^1S–2^3S. Compared with Be III (Fig. 2), the resonance structure has spread out somewhat since the energy-level difference ΔE_i within a given complex of resonances such as $1s3l3l'$ increases as Z. However, the energy differences ΔE_n between the different complexes such as $n=2$ and 3, increase as Z^2; thus with increasing Z the ratio $\Delta E_i/\Delta E_n$ gets smaller. In Fig. 3 we see that the effective averaged cross section just above the 2^3S threshold, represented by the dashed line, is more than six times larger than the background just above the 2^1P^o thresholds. The energy difference between the 2^1S and the 2^3P^o states is indistinguishable in the figure, but a Gailitis-averaged value in this region is calculated and is denoted by $\bar{\Omega}[k^2(2^1S)=0]$. At the 2^3P^o threshold once again we have a large Gailitis jump as described earlier.

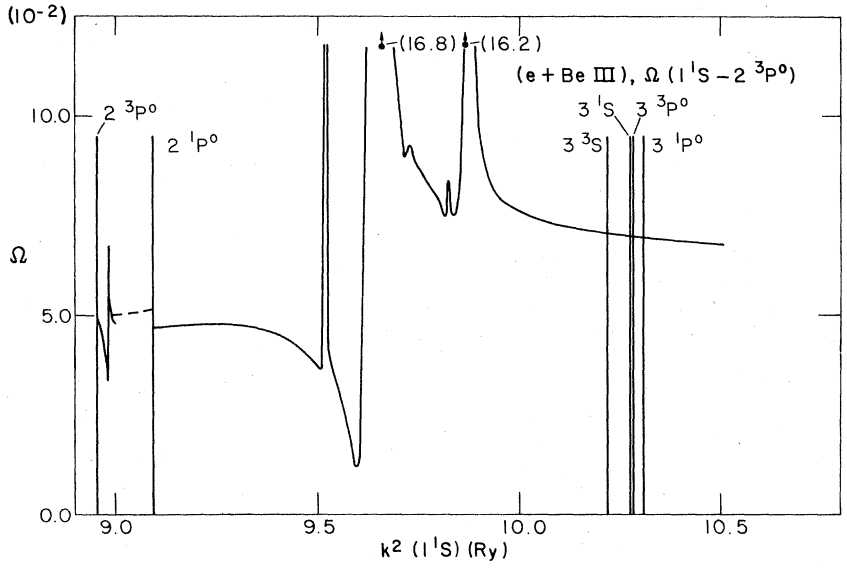

FIG. 4. Collision strength for the intercombination transition 1^1S–2^3P^o in Be III.

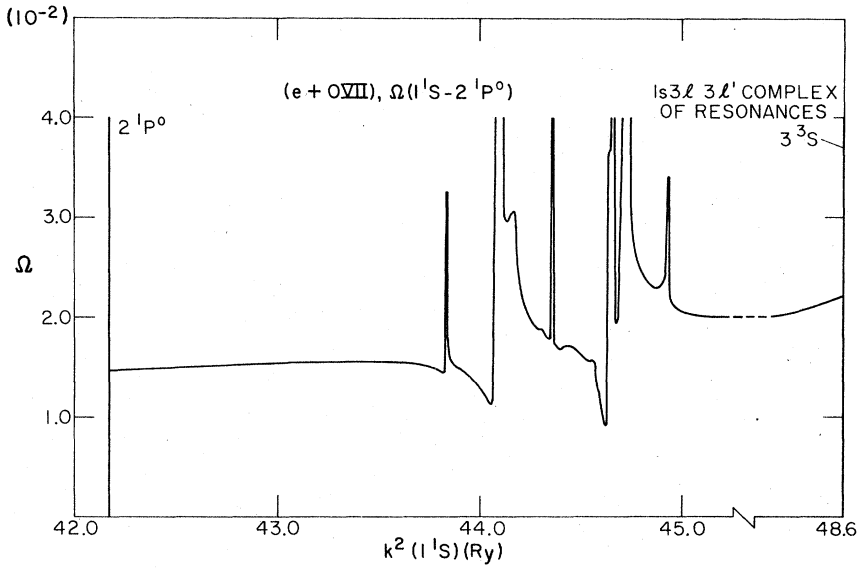

FIG. 5. Collision strength for the optically allowed transition $1^1S-2^1P^o$ in O VII.

In Fig. 4 we have plotted the collision strength for the *intercombination* transition $1^1S-2^3P^o$, and also in Be III. The $1s3l3l'$ group of resonances is shown along with some of the structure above the 2^3P^o threshold; the latter was obtained as before through QDT extrapolation of R matrices from above the 2^1P^o threshold. An important point to notice here is that in the vicinity of the first resonance above the 2^1P^o threshold ($1s3s^2$) the cross section is depressed considerably in comparison with the background cross section near the $n=3$ complex. Finally, in Fig. 5 we plot the collision strength for the *optically allowed* transition $1^1S-2^1P^o$ in O VII. The Z^2 increase accounts for the large energy differences between the different complexes. Also, one sees considerably more structure within the $1s3l3l'$ group (due to the increase with Z) compared to Be III or C V.

The agreement between the present DW calculations and similar close-coupling calculations for cross sections and rates may be assessed by comparing the background collision strengths in the two approximations. In Table V we compare our five-state DW calculations including correlation functions (denoted by 5DW+$3l3l'$, following Hayes and Seaton[13]) with the five-state close-coupling calculations (5CC) by Wyngaarden *et al.*,[22] for C V and O VII. The work of Wyn-

TABLE V. Background collision strengths from present DW and CC (Ref. 22) calculations.

	1^1S-2^3S		1^1S-2^1S		$1^1S-2^3P^o$		$1^1S-2^1P^o$	
Energy (Ry)	5DW	5CC	5DW	5CC	5DW	5CC	5DW	5CC
				C V				
36.0	0.004 14	0.004 51	0.0155	0.0165	0.0202	0.0207	0.0676	0.0765
50.0	0.002 90	0.002 78	0.0185	0.0188	0.0119	0.0111	0.1024	0.1110
67.0	0.001 90	0.001 84	0.0207	0.0204	0.0061	0.0061	0.1391	0.1449
110.0	0.000 86	0.000 83	0.0230	0.0227	0.0021	0.0021	0.2001	0.2049
23.0	0.005 5	0.009 4	0.0064	0.0133	0.0350	0.0397	0.0198	0.0344
				O VII				
45.0	0.003 3	0.003 9	0.0064	0.0070	0.0203	0.0198	0.0208	0.0229
50.0	0.003 1	0.003 3	0.0070	0.0074	0.0180	0.0171	0.0250	0.0276
63.0	0.002 5	0.002 3	0.0080	0.0083	0.012	0.0118	0.0385	0.0389
75.0	0.002 1	0.001 8	0.0097	0.0089	0.0092	0.0086	0.0480	0.0485
126.0	0.001 0	0.000 9	0.0117	0.0106	0.0033	0.0031	0.0817	0.0797
210.0	0.000 46	0.000 4	0.0129	0.0118	0.0012	0.0011	0.1159	0.1131

gaarden *et al.* does not include any resonance structure and therefore comparison is made at energies above the $n = 3$ states where resonances are not included in the present work. The agreement between the two is exceptionally good, the *worst* disagreement being 11.6% for $1\,^1S-2\,^1P^o$ transition in C V at 36.0 Ry. In addition to the background values we have also compared our results for C V at an energy of 23.0 Ry (the row between solid lines) which is just above the $2\,^1P^o$ threshold, and where the differences are considerable (except for the transition $1\,^1S-2\,^3P^o$). This indicates that the difference between our wave functions (including additional correlation functions), and those of Wyngaarden *et al.*, manifests itself largely in the near-threshold region. The presence of resonances would also contribute to the depression of the cross section just above the $2\,^1P^o$ threshold. The effect of using different wave functions is considered in detail by Foster *et al.*[19] In case of O VII, the agreement with the CC values is good at all energies considered. The first energy, 45.0 Ry, lies just above the $1s3l3l'$ group of resonances in O VII. In general, the good agreement between the DW and the CC (Table V), points to the fact that coupling between different states for electron scattering with He-like ions is weak. We may also attribute it to well optimized wave functions being used in both sets of calculations.

Pindzola *et al.*[23] have carried out calculations for electron scattering with O VII including resonance effects in an "attached-excited-target approximation." However, they took into account only a few isolated resonances below the $3\,^3S$ threshold and therefore found the effects to be small. At the $2\,^1P^o$ threshold, Pindzola *et al.* compute the $1\,^1S-2\,^1P^o$ cross section to be about $4.3\times10^{-4}(\pi a_0^2)$ as compared to our value of 3.6×10^{-4} (πa_0^2)—a difference of about 16%. Pindzola *et al.* have also obtained the positions of some of the doubly excited autoionizing states of O VI and these agree with our calculations (Table IV) to well within 1%.

B. Excitation rates

The presence of large numbers of resonances in the cross sections complicates the task of computing excitation rates. Contributions to the total rate parameter γ have to be calculates separately for different energy regions. For example, for each of the three energy intervals described in the previous section we have treated separately three different groups of partial waves; i.e., $l, l' < 4$, where we perform detailed resonance analysis, $4 < l, l' \leq 15$, where we use the DW approximation but no resonance analysis, and $15 < l$, $l' \leq \infty$, where we use the CB approximation. The calculation and the results obtained will be described in detail in a subsequent work (in preparation) for all transitions involving the $n = 2$ states and all ions mentioned before (Sec. I). However, we discuss below certain interesting features of these calculations.

The rate parameter γ defined by (2) consists of an integral of the product of the Maxwellian $e^{-\epsilon/kT}$ with the collision strength $\Omega(\epsilon)$ over all energies ϵ of the scattering electrons. Therefore at a given T the Maxwellian determines the energy range in which $\Omega(\epsilon)$ contributes to $\gamma(T)$. At 10^4K, for instance, *most* of the contribution to γ comes from $\epsilon < 0.1$ Ry, at 10^5 K, from $\epsilon < 1.0$ Ry, and so on. Thus the contribution to γ from the autoionizing resonances at a given T depends on whether or not the resonances are accessible to the Maxwellian. For example, it is clear from Fig. 2 that at 10^4 K the near-threshold resonance structure that greatly enhances the effective cross section relative to the region above the $2\,^1P^o$ threshold, would result in a similar enhancement in γ. This is illustrated in Fig. 6 where we have plotted the rate parameter (2) for the transition $1\,^1S-2\,^3S$ in Be III, versus T [note that in accordance with Eq.

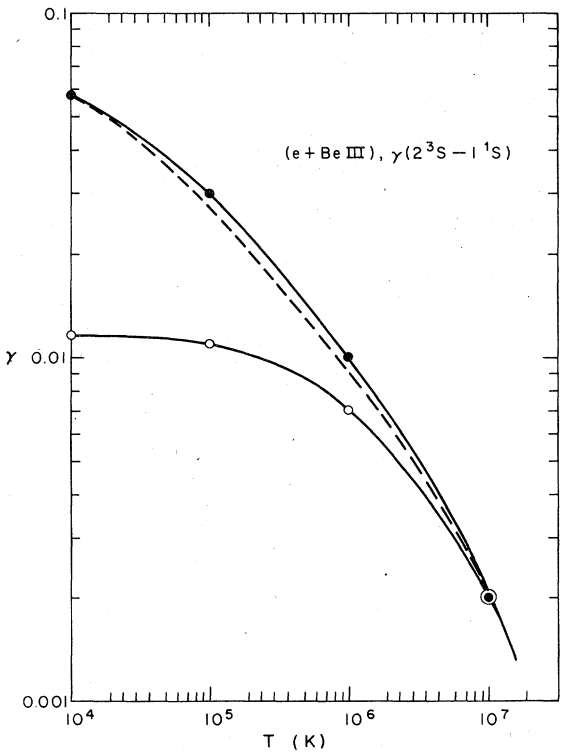

FIG. 6. Rate parameter $\gamma(2\,^3S-1\,^1S)$ for Be III . -●- with resonances, -o- without resonances, --- without the contribution from the $1s3lnl'$ group of resonances.

(2) we write $\gamma_{ji} \equiv \gamma(j-i)$, where j is the upper level]. The lower solid curve is obtained on using only the background collision strength in (2) while the upper solid curve includes all resonance structures (as shown in Fig. 2). There is approximately a factor of 5 difference between the two curves at 10^4K, and even at 10^6 K the effect of the resonances is to increase γ by about 50%.

The dashed curve in Fig. 6 represents the γ obtained on neglecting the $1s3l3l'$ group of resonances; its contribution is found to be small. Also, since the energy difference between the $1s3l3l'$ group and the $n=3$ complex is very small in Be III, we expect that the contribution from all resonances below the $n=3$, i.e., $1s3lnl'$ for $n>3$, would also be small. However, as the charge on the target ion increases and the energy difference between the different complexes increases as Z^2, we expect the contribution from the $1s3lnl'$ resonances to increase with Z. We estimate the contribution from the entire $1s3lnl'$ series by computing numerically averaged collision strengths over the $1s3l3l'$ complex and extrapolating this average up to the $n=3$ complex. For high Z the necessity of accounting for all resonances converging on to the $n=3$ states may be seen from the example of Fe XXV. As the energy difference between the $n=2$ and complexes is about 86 Ry, the $1s3lnl'$ resonances would make a significant contribution to γ in the 10^6–10^8-K range (e.g., see Fig. 7).

The ratio of the resonant contribution to the nonresonant background depends on the type of transition and the magnitude of the background cross section. For the optically allowed transitions the ratio is much smaller than for the forbidden or the intercombination transitions because the ratio of the cross section due to the background potential scattering for the allowed transitions (dipole type) to the cross section for resonant scattering is much greater than that for the forbidden or intercombination (electric-quadrupole-and magnetic-dipole-type) transitions. As in Fig. 6, in Figs. 7 and 8 we plot rate parameters for the intercombination transition $2^3S-2^1P^o$ and the allowed transition $1^1S-2^1P^o$ in Fe XXV. In the cross sections for both of these transitions the resonant contribution is almost entirely from the $1s3lnl'$ group. The maximum resonance enhancement of $\gamma(2^1P^o-2^3S)$ is approximately a factor of 6 at about 10^7 K, whereas in $\gamma(2^1P^o-1^1S)$ it is only about 15%. In Be III, for $\gamma(2^3S-1^1S)$ (Fig. 6), most of the resonance contribution results from the $1s2lnl'$ complex that lies just above the excitation threshold and therefore does not affect the rate parameter at high T ($T>10^7$ K). In Fig. 8 we have a similar situation but this is because at high T most of the contribution to γ comes from Ω at high energies where resonances have been neglected. For $\gamma(2^1P^o-2^3S)$ (Fig. 7), however, the resonance enhancement remains roughly constant as we go to higher T since for this transition Ω decreases rapidly with increasing energy, and most of the contribution to γ comes from the lower-energy range $\epsilon < E(3^3S)$, where we have a large contribution from resonances. The collision strengths decrease with energy for the forbideen and the intercombination transitions and

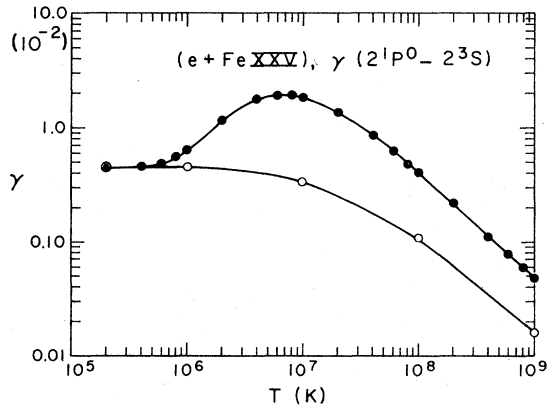

FIG. 7. Rate parameter $\gamma(2^3S-2^1P^o)$ for Fe XXV.

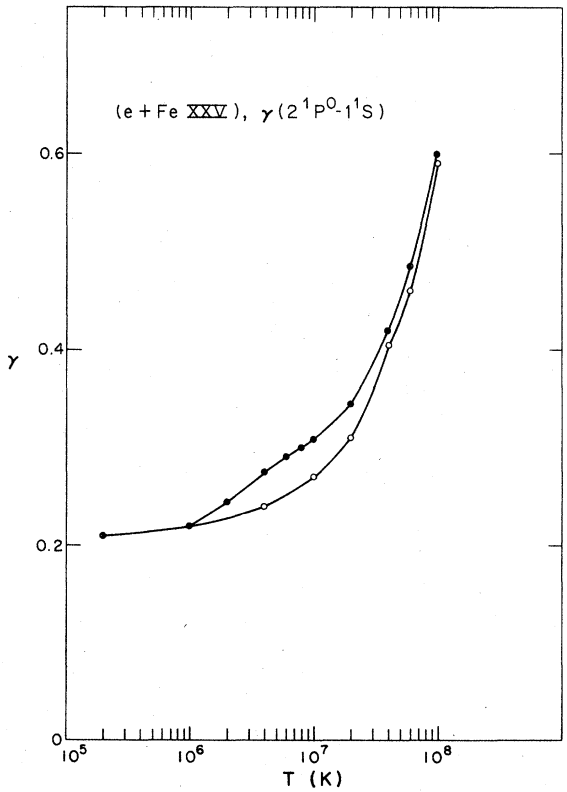

FIG. 8. Rate parameter $\gamma(2^1P^o-1^1S)$ for Fe XXV.

increase with energy for the allowed transition (since the partial-wave sum for the latter converges very slowly). Therefore, the rate parameters $\gamma(2^3S-1^1S)$ and $\gamma(2^1P^o-2^3S)$ decrease with T, whereas $\gamma(2^1P^o-1^1S)$ increases with T.

Wyngaarden *et al.*[22] have computed the rate coefficients q_{ij}[Eq. (1)] for transitions from the ground state 1^1S to the $n=2$ states for several He-like ions. Their values for O VII at 10^6 K for $q(1^1S-2^3S)$, $q(1^1S-2^1S)$, $q(1^1S-2^3P^o)$, and $q(1^1S-2^1P^o)$ are 4.73×10^{-14}, 8.52×10^{-14}, 2.16×10^{-13}, and 2.89×10^{-13} cm^3 sec^{-1}, respectively. Our q values for these transitions are 10.29×10^{-14}, 9.42×10^{-14}, 2.95×10^{-13}, and 2.63×10^{-13} cm^3 sec^{-1}, respectively. The resonances enhance the rates for the 1^1S-2^3S transition by a factor of more than 2. Resonance contributions to $q(1^1S-2^1S)$ and $q(1^1S-2^3P^o)$ are also significant. For the allowed transition $1^1S-2^1P^o$ we do not expect the resonances to make a significant contribution; our q value is actually somewhat lower than that of Wyngaarden *et al.*, but this can probably be attributed to the difference in wave functions and computational algorithm.

Deexcitation rate coefficients for the $2^3S-2^3P^o$ transition in several He-like ions have been determined experimentally by Englehardt *et al.*[24] by observing the $2^3P^o_{0,1,2}-2^3S$ line-intensity ratios. Their measured values are in good agreement with the Coulomb-Born calculations of Blaha[25] and in even better agreement with the present calculations. For C V at 1.7×10^6 K, the values for $q(2^3P^0-2^3S)$ in cm^3 sec^{-1} are 1.34×10^{-12} Engelhardt *et al.*, 1.15×10^{-12}, Blaha, and 1.53×10^{-12}, present work; and for O VII at 2.3×10^6 K, these values are 8.58×10^{-11}, 6.50×10^{-11}, and 7.20×10^{-11}, respectively. Thus for C V and O VII our values differ from the experimental values by only about 15%. However, we must point out that this agreement may be largely fortuitous since the experimental values have error margins of more than a factor of 2.

In general we estimate about 5–10% error in the computed rate parameter due to inaccuracies in the fitting approximations that we have used for the collision strengths. Two other sources of error are in the collision strengths themselves and in our assumption that the averaged resonant contribution below the $n=3$ states remain constant. We have already shown that our background collision strengths agree well with the close-coupling values, and so we expect no more than 10–15% error in γ due to this difference. It is known from a number of previous calculations[26] that the cross section averaged over rydberg series of resonances is smoothly varying and can usually be approximated by a linear function, provided that the $\underline{R}$ matrices just above the threshold are also smoothly varying with energy. In the present case, there are no resonances just above the $n=3$ states and hence, we do not expect any rapid variations with energy in the averaged cross section below. It should be noted that we have not assumed that the averaged cross section is constant, but that the *difference* between the averaged and the background cross sections is constant, i.e., that both behave with energy in a similar manner. Estimating an error up to 10% due to this approximation above, we place the maximum uncertainty in the total computed rate parameters to be 30%.

A source of error not included in the above estimate is the correlation of the $ls3l3l'$ group of autoionizing states with the higher members of the rydberg series $1s3lnl'$ and the resulting effect on the positions and widths of the former. We expect this effect to diminish with increasing Z. Another unevaluated source of error is the departure from LS coupling with increasing Z. Intercombination transitions involving the state $^3P^0$ are the most affected. Jones[27] has shown that this effect is significant for ions with $Z > 20$. In particular, for Fe XXV the collision strength $\Omega(1^1S-2^3P^o)$ is increased by 6% at the energy $k^2(1^1S)=493.3$ Ry and by 18% at 676 Ry, when the intermediate coupling effects are included.

VI. CONCLUDING REMARKS

In this work we have described calculations for electron scattering with He-like ions employing the distorted-wave approximation, and have studied resonances in the cross sections and their effect on the excitation-rate coefficients. The analysis of resonances between the $n=2$ states was carried out using quantum-defect theory, as incorporated in the program RANAL.[14] As such it was not peculiar to the distorted-wave approximation used in the present work, but could have been carried out using $\underline{R}$ matrices computed in any approximation. Resonances above the $n=2$ states were obtained by including carefully chosen correlation functions in the expansion for the total trial wave function, and our results suggest that this technique is a very powerful extension of the conventional distorted-wave approximation.

It has been shown in the present work that the resonance contribution to the excitation rates is expected to very important, particularly for the forbidden and the intercombination transitions.[28] As an example, consider the transition 1^1S-2^3S in Be III, C V, O VII, and Fe XXV. We find that the ratio of the computed rate parameter to the rate parameter neglecting resonances is roughly 4.4 for Be III, 5.8 for C V, 3.8 for O VII, and 1.8 for Fe XXV at $T/Z^2=10^3$. We conclude

that previous analyses of laboratory and astrophysical plasmas employing line ratios for He-like ions may have to be reexamined.

It has been pointed out by Presnyakov and Urnov[6] that the enhancement in the electron-impact excitation cross sections due to the autoionizing resonances is reduced when dielectronic recombination effects are taken into account. For highly charged ions this is particularly true since the ratio of the radiative transition probability to the autoionization probability increases as Z^4. A theoretical treatment has been worked out by Seaton and Bell (M. J. Seaton, private communication). At present, work is in progress to include dielectronic recombination effects on the scattering cross section for the He-like ions.

The present calculations should be the most accurate nonrelativistic calculations to date. However, for highly ionized ions it may prove necessary to take into account the departure from pure LS coupling. Also, the fine-structure transitions within the $n = 2$ complex are of astrophysical interest and computations in intermediate coupling for such transitions are planned.

ACKNOWLEDGMENTS

This work was supported in part by the U. S. Department of Energy (Office of Basic Energy Sciences). The computer code used for the Coulomb-Bethe calculation was written by Dr. A. Burgess and Dr. V. B. Sheorey. Part of the work was done using computer time granted by the National Center for Atmospheric Research. We would like to thank Dr. Helen Mason and Dr. Hugh Summers for correspondence regarding astrophysical applications of this work. We would also like to thank Professor M. J. Seaton for discussion.

---

*Staff members, Quantum Physics Division, National Bureau of Standards, Boulder, Colorado 80309.

[1]A. H. Gabriel and C. Jordan, Nature 221, 947 (1969); Mon. Not. R. Astron. Soc. 145, 241 (1969).
[2]G. R. Blumenthal, G. W. F. Drake, and W. H. Tucker, Astrophys. J. 172, 205 (1972).
[3]H. P. Summers and R. W. P. McWhirter, J. Phys. B 12, 2387 (1979).
[4](a) A. Burgess, D. G. Hummer, and J. A. Tully, Philos. Trans. R. Soc. London 226, 225 (1970); (b) A. Burgess, J. Phys. B 7, L364 (1974).
[5]M. J. Seaton, Adv. At. Mol. Phys. 11, 83 (1975).
[6]L. P. Presnyakov and A. M. Urnov, J. Phys. B 8, 1280 (1975).
[7]M. J. Seaton, J. Phys. B 2, 5 (1969).
[8]W. Eissner and M. J. Seaton, J. Phys. B 5, 2187 (1972).
[9]W. Eissner, in *Proceedings of the Seventh ICPEAC, Amsterdam, 1971,* edited by T. Govers and F. J. De Heer (North-Holland, Amsterdam, 1972), p. 460.
[10]P. G. Burke and M. J. Seaton, Methods Comput. Phys. 10, 1 (1971).
[11]W. Eissner, M. Jones, and H. Nussbaumer, Comput. Phys. Commun. 8, 270 (1974). The explicit form of $V(\lambda_l, r)$ is given by W. Eissner and H. Nussbaumer, J. Phys. B 2, 1028 (1969).
[12]P. G. Burke and A. J. Taylor, J. Phys. B 2, 44 (1969).
[13]M. A. Hayes and M. J. Seaton, J. Phys. B 11, L79 (1978).
[14]A. K. Pradhan and M. J. Seaton (unpublished).
[15]A. W. Weiss, J. Res. Natl. Bur. Stand. Sect. A 71, 163 (1967).
[16]A. M. Ermolaev and M. Jones, J. Phys. B 7, 199 (1974).
[17]J. L. Fox and A. Dalgarno, Phys. Rev. A 16, 283 (1977).
[18]E. Holoien and S. Geltman, Phys. Rev. 153, 81 (1967).
[19]G. Foster, D. G. Hummer, and D. W. Norcross (unpublished).
[20]A. Burgess and V. B. Sheorey, J. Phys. B 7, 2403 (1974).
[21]P. O. Taylor, R. A. Phaneuf, and G. H. Dunn (unpublished).
[22]W. L. Wyngaarden, K. Bhadra, and R. J. W. Henry, Phys. Rev. A 20, 1409 (1979).
[23]M. S. Pindzola, A. Temkin, and A. K. Bhatia, Phys. Rev. A 19, 72 (1979).
[24]W. Engelhardt, W. Köppendörfer, and J. Sommer, Phys. Rev. A 6, 1908 (1972).
[25]M. Blaha, as quoted in Ref. 24.
[26]A. K. Pradhan, J. Phys. B 9, L133 (1976); Mon. Not. R. Astron. Soc. 184, L133 (1976).
[27]M. Jones, Mon. Not. R. Astron. Soc. 169, 211 (1974).
[28]The literature on electron-impact excitation of He-like ions is, of course, much larger than the few papers cited herein particularly in support of this point. The reader is referred to Refs. (22) and (23) for some additional citations of earlier work and to the detailed review article by R. J. W. Henry (unpublished).